

A copper–thiolate polynuclear cluster in the ACE1 transcription factor

(metallothionein/metal sensor/metal cluster/gene regulation)

C. T. DAMERON*, D. R. WINGE*, G. N. GEORGE†, M. SANSONE†, S. HU‡, AND D. HAMER‡§

*University of Utah Medical Center, Salt Lake City, UT 84132; †Exxon Research and Engineering Co., Annandale, NJ 08801; and ‡Laboratory of Biochemistry, National Cancer Institute, National Institutes of Health, Bethesda, MD 20892

Communicated by Maxine F. Singer, April 15, 1991 (received for review January 17, 1991)

ABSTRACT ACE1 is the transcriptional activator of the metallothionein (*CUP1* locus) gene in *Saccharomyces cerevisiae*. Previous data had implicated the N-terminal domain of ACE1 as responsible for the Cu-dependent specific DNA binding. An expression system in *Escherichia coli* was constructed to enable the isolation of an ACE1 domain containing the DNA and Cu-binding regions. Here we report the purification and characterization of the Cu–ACE1 truncated molecule. Spectroscopic techniques showed that ACE1 contains an unusual type of DNA binding structure that is based on a polynuclear Cu(I)–cysteiny l thiolate cluster. The cluster consists of six or seven Cu(I) ions coordinated to cysteiny l thiulates in a trigonal geometry distorted from planarity. The Cu(I)–cysteine cluster of Cu–ACE1 exhibits structural properties analogous to the Cu(I)–thiolate polynuclear cluster in yeast Cu–metallothionein itself, suggesting an unusual mechanism for the evolution of this regulatory factor. The Cu cluster organizes and stabilizes the conformation of the N-terminal domain of ACE1 for specific DNA binding.

Sequence-specific DNA-binding proteins play key roles in the expression and transmission of genetic material. Many of these proteins share common structural motifs—such as the helix–turn–helix, leucine zipper, and zinc finger—that position the specific DNA-binding residues in appropriate juxtaposition to the target DNA sequence (1). The ACE1[¶] transcription factor, which activates transcription of the metallothionein (MT) gene in *Saccharomyces cerevisiae* in response to Cu ions, is not obviously homologous to any of the known DNA binding factors (2–4). Previous biochemical and genetic experiments implicated the N-terminal 122 amino acids of ACE1 in specific DNA binding (2–6). This region of the protein bears several sequence similarities to yeast MT including the presence of 12 cysteiny l residues of which 10 are arranged in Cys–Xaa–Cys or Cys–Xaa–Xaa–Cys pairs and limited numbers of hydrophobic residues (2–4). Yeast MT contains a Cu(I)–cysteiny l thiol polynuclear cluster that provides the energy of stabilization for the tertiary fold (7, 8). The similarity of ACE1 and MT led to the prediction that the active form of ACE1 contained a Cu(I) cluster (2).

The role of Cu in the function of ACE1 was confirmed by studies on ACE1 produced as a fusion protein in *Escherichia coli* or in an *in vitro* translation system. These studies suggested that the specific interaction of ACE1 and DNA promoter sequences in the MT gene was dependent on the presence of Cu or Ag ions (2, 5). The addition of the Cu(I) chelator KCN, which depletes MT of bound Cu ions, abolished the specific interaction of Cu–ACE1 and DNA.

To determine the nature of the Cu–ACE1 complex, an *E. coli* expression system was constructed for use in the puri-

fication of a truncated form of ACE1 containing the N-terminal 122 amino acids. Here we provide biophysical evidence that Cu–ACE1 contains a Cu(I)–cysteiny l thiolate polynuclear cluster.

MATERIALS AND METHODS

Expression and Purification of Cu–ACE1. The ACE1 expression system was constructed by converting the initiation codon of the ACE1 gene into a *Nco* I site by site-directed mutagenesis. A *Nco* I/*Bgl* II fragment encoding the first 122 amino acids of ACE1 was subcloned into the T7 expression plasmid Pet3D (9), resulting in the fusion of ACE1(1–122) with the following T7 sequence at the C terminus: ADPAANKARKEAELAAATAEQ. A BL21 (DE3):pLysS lysogen carrying the recombinant plasmid was grown to late logarithmic phase and treated for 3 h with 0.4 mM isopropyl β -D-thiogalactopyranoside and 1 mM CuSO₄. In the purification of Ag–ACE1, CuSO₄ was omitted from the growth medium and 0.3 mM AgNO₃ was added to the clarified extract. The Cu–ACE1 protein was purified from a freeze–thawed extract clarified by centrifugation. The bulk of the copper was isolated from the crude extract by a 30–50% saturation of ammonium sulfate cut. The precipitate was resuspended in 20 mM potassium phosphate (pH 7.8) containing 1% 2-mercaptoethanol and diluted to a conductivity of 10 mmho for application to a 150-ml heparin/agarose column. Elution was with an 800-ml gradient of 0–1.2 M KCl in 20 mM potassium phosphate buffer containing 4 mM dithiothreitol. The copper-containing fractions eluting near 0.7 M KCl were pooled, brought to 0.8 M in (NH₄)₂SO₄, and applied to a 15-ml phenyl-Sepharose column. The (NH₄)₂SO₄ concentration of the effluent, which contained 80% of the copper, was increased to 1.5 M and reapplied to phenyl-Sepharose. The column was eluted with decreasing amounts of (NH₄)₂SO₄. The Cu-containing fractions were concentrated by ultrafiltration on an Amicon PM-10 membrane, desalted by gel filtration on Sephadex G-25 equilibrated in 20 mM potassium phosphate, pH 7.8/0.1 M NaCl, and stored anaerobically at –70°C.

Preparation of ApoACE1 and Cu Reconstitution. ApoACE1 was prepared by acidification of the Cu–ACE1 protein as described for the preparation of apoMT from Cu–MT (10). The acidified sample was chromatographed on Sephadex G-25 equilibrated with 0.02 M HCl. The demetallized protein was reduced with 100 mM dithiothreitol in 6 M guanidinium hydrochloride/0.01 M EDTA/0.2 M Tris-HCl, pH 8.6. After incubation at 65°C for 1 h, the sample was acidified to pH 1 and chromatographed on Sephadex G-25 equilibrated with 0.02 M HCl. The extent of reduction was assessed by

Abbreviations: MT, metallothionein; EXAFS, extended x-ray absorption fine structure.

§To whom reprint requests should be addressed.

¶ACE1 is also known as CUP2.

quantitation of thiols with dithiodipyridine (11) and protein by amino acid analysis. ApoACE1 samples used for metal reconstitution studies contained at least 97% of the cysteines as reduced thiols.

Cu reconstitution was performed anaerobically as described (10). The Cu(I) stock solution was stabilized as $[\text{CuCl}_2]^-$ prepared by anaerobically dissolving CuCl in 0.01 M HCl containing 1 M NaCl. The excess chloride suppresses disproportionation of Cu(I).

Protein Characterization. Amino acid analysis was performed after hydrolysis of samples in 5.7 M HCl at 110°C for 24 h on a Beckman 6300 analyzer. Quantitation of ACE1 was by quantitative amino acid analysis. Edman degradation was carried out on an Applied Biosystems 475 sequencer with on-line high-performance liquid chromatography analysis of phenylthiohydantoin derivatives. Metal analysis was made by atomic absorption spectroscopy on a Perkin-Elmer 305A instrument.

Spectroscopic Analysis of Cu-ACE1. Absorption spectra were recorded on a Beckman DU 65 recording spectrophotometer and luminescence spectra on a Perkin-Elmer 650-10S fluorimeter (10). For both absorbance and luminescence measurements, the samples were prepared in 0.1 M potassium phosphate (pH 6.5). X-ray absorption spectra were recorded on the Exxon extended x-ray absorption fine structure (EXAFS) beamline X10-c at the national synchrotron light source at the Brookhaven National Laboratory. The $\text{CuK}\alpha$ x-ray fluorescence emission was measured with a 13-element Ge detector. Samples were prepared as frozen solution in 20 mM potassium phosphate (pH 6.5) containing 10% (vol/vol) glycerol and were measured at 4 K in an Oxford Instrument CF1204a liquid helium flow cryostat. EXAFS curve fitting was carried out as described (8), except that improved theoretical curved wave phase and amplitude functions were calculated by using the program FEFF (12, 13).

RESULTS

The *E. coli* phage T7 expression system (9) was used to overproduce a 141-amino acid peptide that contains the N-terminal 122 amino acids of ACE1 and 19 C-terminal amino acids from the vector. This 141-residue polypeptide was purified to homogeneity by a combination of ion-exchange and hydrophobic interaction chromatography from cells induced in the presence of CuSO_4 . Amino acid analysis of the purified Cu-ACE1 after 6M HCl hydrolysis revealed a composition identical to that predicted from the nucleotide sequence. A single major band was observed on SDS/PAGE at an apparent M_r of 19,953 with additional lower molecular weight components. Sequence analysis by Edman degradation for 10 cycles revealed the ACE1 sequence MV-VINGVKYA with a 65% first-step yield. In the first three cycles, the cited residues accounted for >90% of the total pmol of phenylthiohydantoin-derivatized amino acids in the chromatogram. Sequence analysis of the lower molecular weight bands blotted onto polyvinyl membranes revealed the same ACE1 N-terminal sequence, implying that the heterogeneity arose at the C terminus of ACE1.

Cu copurified with the ACE1 molecule throughout the purification procedures, even in the presence of high levels of competing thiols used to maintain a reducing environment. Samples from multiple isolates contained molar Cu/polypeptide ratios between 4 and 9. In the isolation of Ag-ACE1, the Ag(I)-binding stoichiometry varied from 4 to 8. The variation observed relates to the copurification of ACE1 molecules with various degrees of Cu saturation arising from the heterologous expression system. These Cu-ACE1 samples purified from *E. coli* will be designated as native Cu-ACE1.

An optical transition in the UV near 260 nm was observed in native Cu-ACE1 samples regardless of the Cu stoichiometry, which is characteristic of Cu-S charge transfer bands (Fig. 1). The shoulder feature in the UV spectrum was abolished by treatment of the sample with the Cu(I) chelator KCN or acidification of the sample. Acid conditions of pH < 2 were required for half depletion of the charge transfer bands. Yeast CuMT also exhibits the characteristic 260-nm shoulder transition that is stable to pH conditions down to pH 2 (7, 10).

An unusual spectroscopic feature of Cu-MT is its luminescence at room temperature (10). This emission is indicative of Cu(I) coordination in an environment shielded from solvent interactions; Cu(I)-thiolate clusters formed with small thiolate ligands exhibit luminescence only in the frozen state and Cu(II) complexes are not luminescent (10, 14, 15). Excitation of Cu-ACE1 with UV light yielded a similar emission band with a wavelength maximum of 580 nm and an excitation wavelength maximum at 310 nm (Fig. 1 *Inset*). As also found for Cu-MT, the luminescence was partially quenched by O_2 and to a lesser extent by acrylamide (data not shown) and was eradicated at a pH below 1 or in the presence of KCN (Fig. 1 *Inset*).

Cu reconstitution studies were carried out to verify the maximal binding stoichiometry. Samples of apoACE1 titrated with increasing quantities of Cu(I) revealed an increase in the UV absorbance as a function of added metal (Fig. 2A). The spectrum was dominated by a shoulder near 260 nm characteristic of Cu-thiol charge transfer transitions. The shoulder feature was clearly visible in samples containing up to 6 mol equivalents (eq) of Cu(I). At higher Cu(I) levels, the shoulder was abolished and the slope of the absorbance increase as a function of added metal changes (Fig. 2A *Inset*). Luminescence emission increased with increasing Cu(I) equivalencies peaking at 6 mol eq of Cu(I). The decrease in emission at higher Cu(I) equivalents is observed in titrations of Cu-MT and has been interpreted as disruption of the

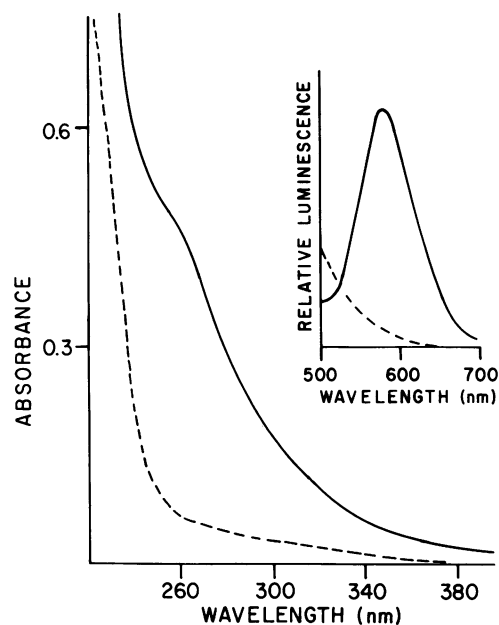


FIG. 1. Optical properties of Cu-ACE1. The UV absorption spectra of Cu-ACE1 (0.125 mg/ml) was recorded for a sample in 0.2 M potassium phosphate (pH 7) (—) and a sample incubated within the same buffer with 5 mM KCN (---). The KCN spectrum was recorded as a difference spectrum of KCN-treated ACE1 and a buffer blank containing 5 mM KCN and Cu(I) (4.8 $\mu\text{g/ml}$). Cu(I)- CN_x absorbs in the UV. (*Inset*) Emission spectrum of Cu-ACE1 (—) and Cu-ACE1 treated with 5 mM KCN (---) at the excitation maximum of 310 nm.

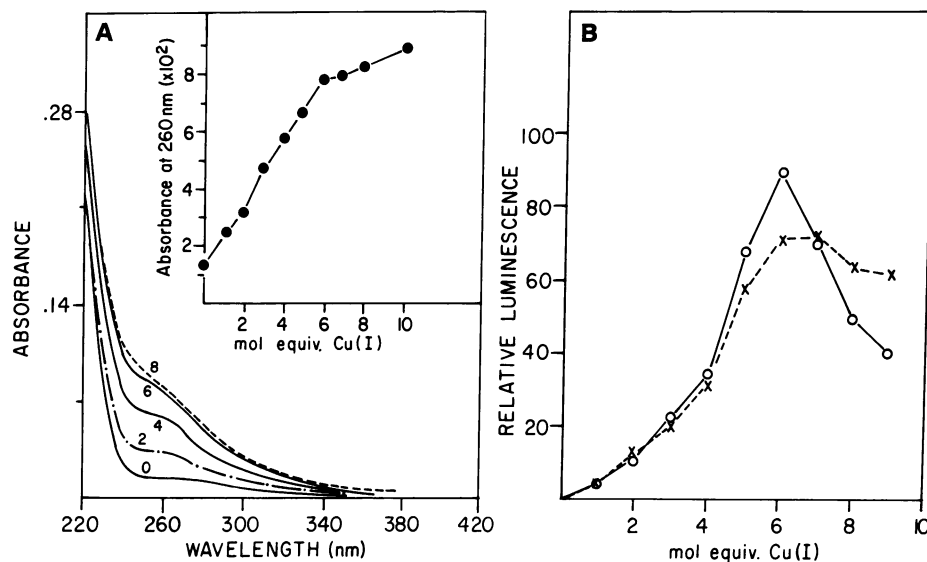


FIG. 2. Cu reconstitution of apoACE1. Samples of apoACE1 (1.87 nm/ml) were titrated anaerobically with increasing mol eq of Cu(I). The samples were scanned for UV absorbance (A) and luminescence (B). The spectra of samples containing even integers of mol eq of Cu(I) are shown, whereas the absorbances at 260 nm of samples with 0–10 mol eq of Cu(I) are plotted in the *Inset*. The numbers on the spectral curves represent the mol eq of added Cu(I). The intensity of the emission peak at 580 nm was recorded for each of the same samples with excitation at 310 nm. Emission was recorded for samples in the absence (—) and presence (---) of 100 nmol of cysteine to minimize the destabilization of the molecule due to excess Cu(I). A stabilizing effect of thiols on emission is observed with Cu-MT (10).

cluster structure (10). In the presence of added cysteine, peak emission is seen between 6 and 7 mol eq of Cu(I).

X-ray absorption spectroscopy was used to obtain a more detailed picture of the Cu coordination. Analysis was carried out on native Cu-ACE1, reconstituted Cu₄-ACE1 and Cu_{6,8}-ACE1 molecules. The x-ray absorption edge spectra of these samples together with Cu-MT are shown in Fig. 3A. All the

spectra are quite similar, possessing no visible 1s → 3d transition near 8980 eV (1 eV = 1.602 × 10⁻¹⁹J), confirming a Cu(I) oxidation state. The shoulder that is present close to 8984 eV in each sample is suggestive of Cu(I) with a trigonal coordination environment (17). The broadening of this feature accompanies a significant distortion of the copper coordination from a trigonal planar geometry (8, 17, 18).

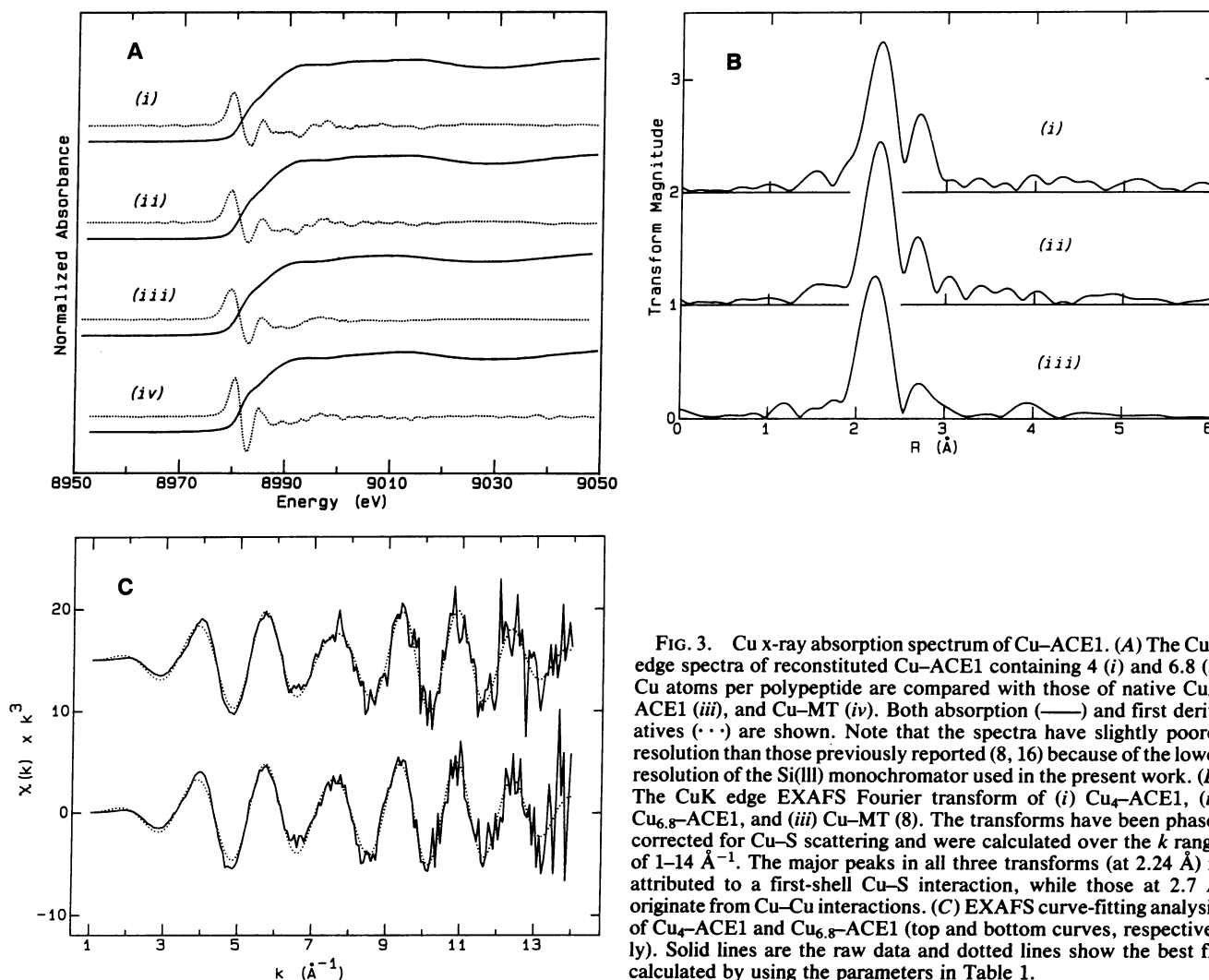


FIG. 3. Cu x-ray absorption spectrum of Cu-ACE1. (A) The CuK edge spectra of reconstituted Cu-ACE1 containing 4 (i) and 6.8 (ii) Cu atoms per polypeptide are compared with those of native Cu₄-ACE1 (iii), and Cu-MT (iv). Both absorption (—) and first derivatives (· · ·) are shown. Note that the spectra have slightly poorer resolution than those previously reported (8, 16) because of the lower resolution of the Si(III) monochromator used in the present work. (B) The CuK edge EXAFS Fourier transform of (i) Cu₄-ACE1, (ii) Cu_{6,8}-ACE1, and (iii) Cu-MT (8). The transforms have been phase-corrected for Cu-S scattering and were calculated over the *k* range of 1–14 Å⁻¹. The major peaks in all three transforms (at 2.24 Å) is attributed to a first-shell Cu-S interaction, while those at 2.7 Å originate from Cu-Cu interactions. (C) EXAFS curve-fitting analysis of Cu₄-ACE1 and Cu_{6,8}-ACE1 (top and bottom curves, respectively). Solid lines are the raw data and dotted lines show the best fit calculated by using the parameters in Table 1.

Table 1. Parameters calculated from unrestricted curve fitting of reconstituted Cu-ACE1 samples

| Sample | Cu-S | | | Cu-Cu | | |
|-----------------------|----------|--------------|-----------------------------|----------|--------------|-----------------------------|
| | <i>N</i> | <i>R</i> , Å | σ^2 , Å ² | <i>N</i> | <i>R</i> , Å | σ^2 , Å ² |
| Cu ₄ -ACE1 | 3.0 | 2.26 | 0.0040 | 1.1 | 2.68 | 0.0035 |
| Cu ₇ -ACE1 | 2.9 | 2.26 | 0.0032 | 0.8 | 2.68 | 0.0034 |

EXAFS curve fitting yields values for the mean coordination number per Cu (*N*), the mean interatomic distance (*R*), and the mean-square deviation in *R* (σ^2), sometimes called the Debye-Waller factor. The estimates of *N* and σ^2 are considered accurate to $\pm 20\%$. Values for *R* are considered accurate to ± 0.02 Å for directly coordinated ligands (i.e., Cu-S) and to ± 0.04 Å for more distant scatterers (i.e., Cu-Cu).

The copper EXAFS Fourier transforms and the EXAFS best fits from the curve-fitting analyses are shown in Fig. 3. The major interaction in the EXAFS is attributable to a Cu-S interaction, and inclusion of lighter scatterers such as Cu-N did not improve the fit. The outer shell EXAFS, seen as the transform peak at ≈ 2.7 Å in Fig. 3B, could only be fitted to an interaction with a heavy scatter, such as Cu-Cu. The presence of marked Cu-Cu interactions clearly indicates the presence of a copper cluster within the ACE1 protein. The results of unrestricted EXAFS curve fitting of Cu₄-ACE1 and Cu_{6.8}-ACE1 copper EXAFS are summarized in Table 1. In agreement with our interpretation of the edge spectrum, the EXAFS curve-fitting analysis of both Cu₄-ACE1 and Cu_{6.8}-ACE1 gave Cu-S coordination numbers of ≈ 3 , and a Cu-S bond length of 2.26 Å, which is known to be characteristic of copper trigonally coordinated to sulfur (8, 16).

CD was used to compare the secondary structures of Cu-ACE1 and Cu-MT and to study the effects of Cu binding on protein conformation. The CD spectrum of the native Cu-ACE1 discounts any significant amount of periodic secondary structure (Fig. 4). Rather, the spectrum is similar to proteins of compact structure lacking appreciable α -helical or β -strand structures. The bulk structure of Cu-ACE1 appears more organized than that in Cu-MT, as indicated by the greater negative ellipticity. Addition of concentrations of KCN known to deplete the Cu-ACE1 molecule of Cu(I) ions partially diminished the ellipticity, suggestive of some disruption in structure. Nevertheless, apoACE1 retains a greater proportion of structure than either Cu-MT or apoMT. While the stabilization energy of the tertiary fold of Cu-MT is dominated by Cu-thiolate coordinate bonds, the conformation of Cu-ACE1 may be stabilized by Cu-S coordinate

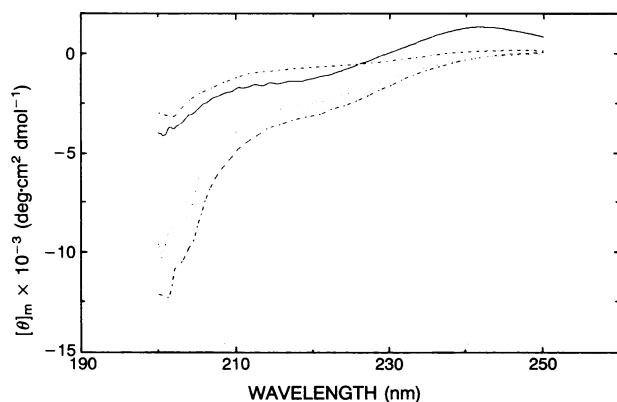


Fig. 4. CD spectroscopy on Cu-ACE1 and Cu-MT. Spectra were recorded on Cu-ACE1 (---), Cu-ACE1 treated with 5 mM KCN (···), Cu-MT (—), and Cu-MT treated with 5 mM KCN (-·-). Cu-ACE1 (1 mg/ml) and Cu-MT (1 mg/ml) were in 10 mM potassium phosphate (pH 7) containing 0.25 M ammonium sulfate. Four spectra were recorded at 23°C in a 1-mm cuvette on a JASCO 20-C for each sample, and the averaged spectrum is presented.

bonds and additional noncovalent interactions. Guanidinium hydrochloride at 1 M resulted in a minimal disruption in structure in Cu-ACE1 but a substantial disruption in KCN-treated Cu-ACE1 as deduced by the CD spectroscopy (data not shown). These data are corroborated by *in vitro* proteolysis experiments using fluorescamine to monitor peptide bond cleavage (7, 19). Cu-ACE1 and Cu-MT samples were largely resistant to digestion with proteinase K at neutral pH, but preincubation of each protein with KCN destabilized the structures so that significant proteolysis was observed.

DISCUSSION

The biophysical data presented here confirm the structural similarity between Cu-ACE1 and the gene product that it regulates, Cu-MT. The principal points of similarity are the presence of multiple Cu(I) ions bound in trigonal coordination to cysteine thiolates in a Cu-S polynuclear cluster. The identification of Cu-S coordination is based on the previous demonstration that cysteinyl residues in ACE1 are required for function (20), the charge transfer transition in the UV, and the fit to the EXAFS Fourier transform data. The confirmation of monovalent Cu ions is based on the observed luminescence at room temperature and the x-ray edge feature at 8984 eV. The presence of a Cu(I)-S polynuclear cluster is indicated by the observed Cu-Cu distance of 2.7 Å and the edge feature in the charge transfer transition in the UV.

The polynuclear cluster is apparent in Cu-ACE1 molecules containing Cu(I) stoichiometries of 4 and 6.8. Cluster formation is expected at substoichiometries if Cu(I) binding to ACE1 occurs in an all-or-nothing manner, as is the case with Cu-MT. The cluster structure appears to maximally contain six or seven Cu(I) ions, although additional Cu(I) ions can bind with apparent disruption of the cluster structure. The Cu(I) ions are trigonally bound to cysteinyl thiolates with an average Cu-S distance of 2.26 Å. This distance and x-ray absorption edge feature at 8985 eV confirm the trigonal geometry of each Cu(I) (17, 18). The broadening of this edge feature in Cu-ACE1 is consistent with a distortion of the copper coordination from a trigonal planar geometry (18). The copper environment in Cu-ACE1 is therefore quite similar to the trigonal Cu(I) coordination in Cu-MT (8, 16).

Cu(I) coordination within ACE1 stabilizes and organizes the tertiary fold of ACE1, as is the situation with MT. The minimal quenching in the emission in both Cu-ACE1 and Cu-MT suggests that the Cu-S cluster in each protein exists within a compact tertiary conformation. The stabilization energy of the tertiary fold in Cu-ACE1 arises in part from the Cu-S coordinate bonds—a situation that exists in Cu-MT. The limited number of aromatic residues in the Cu-binding domain of ACE1 supports the notion of a core Cu-S cluster being an important component of the protein structure. Therefore, the Cu cluster in Cu-MT appears to be a good structural model for the cluster in Cu-ACE1.

Two structural features of Cu-ACE1 may be important for the biology of MT gene regulation. First, the formation of such a polynuclear cluster is expected to be highly cooperative (6, 10, 21). Cooperative cluster formation may allow the cell to respond to a small change in Cu concentration by a large change in gene expression. Second, the presence of a trigonal Cu(I) cluster explains the specificity for metalloregulation of yeast MT gene expression. The only metal ion that forms similar clusters in MT is Ag(I), and this metal ion also activates ACE1 for DNA binding.

The structural similarities between the Cu-ACE1 domain and MT itself suggest that ACE may have evolved by the addition of DNA-binding amino acids to a primordial metal binding structure. The use of metal clusters in signal transduction through transcriptional regulation is one of the diverse strategies in nature to attain specificity in signal re-

sponse. The coordination chemistry of metal clusters may also be important in the metalloregulation of other metabolic pathways.

This work was supported by Research Grant ES 03817 from the National Institutes of Health to D.R.W. The National Synchrotron Light Source is funded by the Division of Materials Sciences, U.S. Department of Energy, under Contract DE-AC02-76CH-0016.

1. Struhl, K. (1989) *Trends Biochem. Sci.* **14**, 137-140.
2. Furst, P., Hu, S., Hacket, R. & Hamer, D. (1988) *Cell* **55**, 705-717.
3. Szczypka, M. & Thiele, D. (1989) *Mol. Cell. Biol.* **9**, 421-429.
4. Welch, J., Fogel, S., Buchman, C. & Karin, M. (1989) *EMBO J.* **8**, 255-260.
5. Buchman, C., Skroch, P., Welch, J., Fogel, S. & Karin, M. (1989) *Mol. Cell. Biol.* **9**, 4091-4095.
6. Furst, P. & Hamer, D. (1989) *Proc. Natl. Acad. Sci. USA* **86**, 5267-5271.
7. Winge, D. R., Nielson, K. B., Gray, W. R. & Hamer, D. H. (1985) *J. Biol. Chem.* **260**, 14464-14470.
8. George, G. N., Byrd, J. & Winge, D. R. (1988) *J. Biol. Chem.* **263**, 8190-8203.
9. Studier, W. F., Rosenberg, A. H., Dunn, J. J. & Dubendorff, J. W. (1991) *Meth. Enzymol.* **185**, 60-89.
10. Byrd, J., Berger, R. M., McMillan, D. R., Wright, C. F., Hamer, D. & Winge, D. R. (1988) *J. Biol. Chem.* **263**, 6688-6694.
11. Grasseti, D. R. & Murray, J. F., Jr. (1967) *Arch. Biochem. Biophys.* **119**, 41-49.
12. Rehr, J. J., Mustre de Leon, J., Zabinski, S. I. & Albers, R. C. (1991) *J. Am. Chem. Soc.*, in press.
13. Mustre de Leon, J., Rehr, J. J., Albers, R. C. & Zabinski, S. I. (1991) *Phys. Rev. B.*, in press.
14. Lerch, K. & Beltramini, M. (1983) *Chem. Scr.* **21**, 109-115.
15. Lytle, F. E. (1970) *Appl. Spectrosc. Rev.* **24**, 319-326.
16. George, G. N., Winge, D. R., Stout, C. D. & Cramer, S. P. (1986) *J. Inorg. Biochem.* **27**, 213-220.
17. Kau, L. S., Spira-Solomon, D. J., Penner-Hahn, J. E., Hodgson, K. O. & Solomon, E. I. (1987) *J. Am. Chem. Soc.* **109**, 6433-6442.
18. Blackburn, N. J., Strange, R. W., Reedijk, J., Volbeda, A., Farooq, A., Karlin, K. D. & Zubieta, J. (1989) *Inorg. Chem.* **28**, 1349-1357.
19. Winge, D. R. (1991) *Methods Enzymol.*, in press.
20. Hu, S., Furst, P. & Hamer, D. (1990) *New Biol.* **2**, 544-555.
21. Good, M., Hollenstein, R., Sadler, P. J. & Vasak, M. (1988) *Biochemistry* **27**, 7163-7166.